③

Clarkson
UNIVERSITY

WALLACE H. COULTER SCHOOL OF ENGINEERING
Technology Serving Humanity

MEMORANDUM

Subject: Progress Report
ULI: FY12 Q2 Progress Report (1/1/2012–3/30/2012)

This document provides a progress report on the project "Advanced Digital Signal Processing" covering the period of 1/1/2012–3/30/2012.

20150309464

William D. Jemison, Professor and Chair, PO Box 5720, Clarkson University, Potsdam, NY 13699-5720
315-268-6509, Fax 315-268-7600, wjemison@clarkson.edu

Background

Backscatter reduction is a critical stage in enhancing the usable range of any hybrid lidar-radar scheme that is deployed into a turbid underwater environment. In a highly scattering environment, many photons reaching the detector will have scattered off particulates in the water, while relatively few photons reaching the detector will have made the round-trip to and from the object of interest. This will cause the system to detect an object whose range is near the volumetric center of the scattering region, rather than the detecting the range to the object of interest.

A similar problem is encountered in the radar areas of moving target indication (MTI) and through-the-wall radar imaging (TWRI), in which radar clutter obscures the desired object return [1,2]. Researchers in these areas have shown that the clutter has lower spatial frequencies than the object, meaning that the clutter return can theoretically be filtered out by a spatial filter without negatively impacting the target return. The backscatter in the turbid underwater environment is analogous to the clutter in these radar scenarios. An early solution to this problem was the use of delay line cancelers, with more recent work focusing on more sophisticated signal processing solutions such as FFT-based filters. The main idea behind the delay line canceler is that the clutter signal is a low frequency signal, which can be attenuated by the high-pass quality of a differentiator. Further modifications can be made to delay line cancelers to fine-tune the behavior, such as widening the clutter rejection region.

Delay Line Cancelers

For proof-of-concept purposes, we have applied two kinds of delay line cancelers to the turbid underwater environment. These two filters and their responses will be briefly characterized, followed by discussion of experimental results achieved with these filters. The simplest filter is the single delay line canceler, shown below in Figure 1. This filter is a simple differentiator which rejects the DC component of the return signal, which is assumed in our scenario to correspond to the scattering contribution of the return. In this filter, the output signal is calculated as the difference between the current input and a spatially delayed previous input:

$$S_{OUT}(z,t) = S_{IN}(z,t) - S_{IN}(z+\Delta z,t)$$

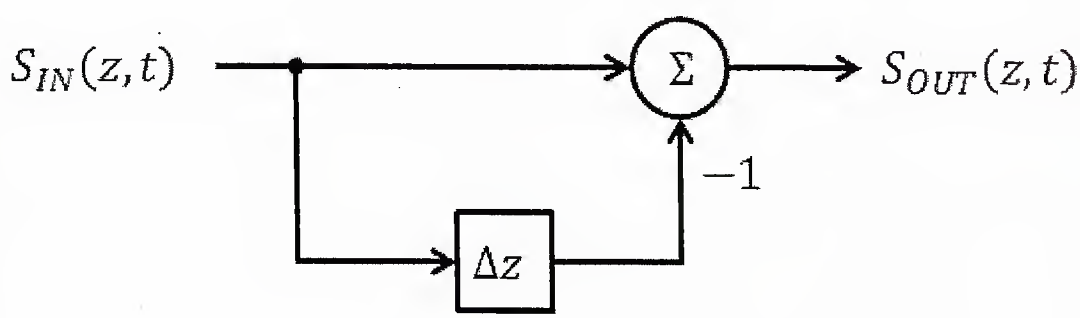

Figure 1. Single delay line canceler

When applying this filtering approach to a turbid underwater environment, the attenuation of such an environment must be taken into consideration. Received power is attenuated according to

$$P = P_0 e^{-cz}$$

where P is the power received by the detector, $P_0$is the power transmitted by the source, c is the beam attenuation coefficient, and z is the distance traveled in the underwater channel. Assuming that the transmitted signal is intensity-modulated with a complex sinusoid, then the input and output signals take the following forms:

$$S_{IN}(z,t) = e^{-cz} e^{j(\omega t - kz)}$$

$$S_{OUT}(z,t) = S_{IN}(z,t) - e^{-c\Delta z} S_{IN}(z,t)$$

where $\omega = 2\pi f$ is the frequency and $k = \frac{2\pi}{\lambda}$ is the spatial frequency of the signal. With this choice of an input signal, the system transfer function H can be shown to be

$$H(\Delta z, c) = 1 - e^{-c\Delta z} \cos(k\Delta z) + je^{-c\Delta z} \sin(k\Delta z)$$

The single delay line filter's dependency on the underwater environment is emphasized by the parameterization on the attenuation coefficient c. If c is changed, then the filter's transfer function will also change even when the spatial delay Δz is held constant. This implies that the filter will need to be tuned for optimal operation in different turbidities. The magnitude and phase responses of the filter can be shown to be

$$M(\Delta z, c) = \sqrt{1 + e^{-2c\Delta z} - 2e^{-c\Delta z} \cos(k\Delta z)}$$

$$\Phi(\Delta z, c) = \operatorname{atan}\left(\frac{e^{-c\Delta z} \sin(k\Delta z)}{1 - e^{-c\Delta z} \cos(k\Delta z)}\right)$$

The magnitude and phase responses for this filter are plotted in Figure 2 and Figure 3, respectively, for selected values of c. The horizontal axis is shown as a factor of the transmitted signal's wavelength. Note that for the extreme case $c = 0$, the filter response reduces to the classical single delay line filter known in the radar community, which is periodic with period λ and suggests an optimal delay of $\Delta z_{opt} = \frac{\lambda}{2}$, in the sense that this is the first point at which point the signal magnitude is most amplified. On the other extreme, as c becomes large, the filter converges towards a high-pass filter with a relatively flat passband region. Additionally, as c increases, the optimal delay is shifting below $\frac{\lambda}{2}$ while the gain at this optimal point is decreasing from the gain in the $c = 0$ case. The optimal delay for selected values of c is summarized in Table 1, along with the magnitude gain and phase shift at these delay points.

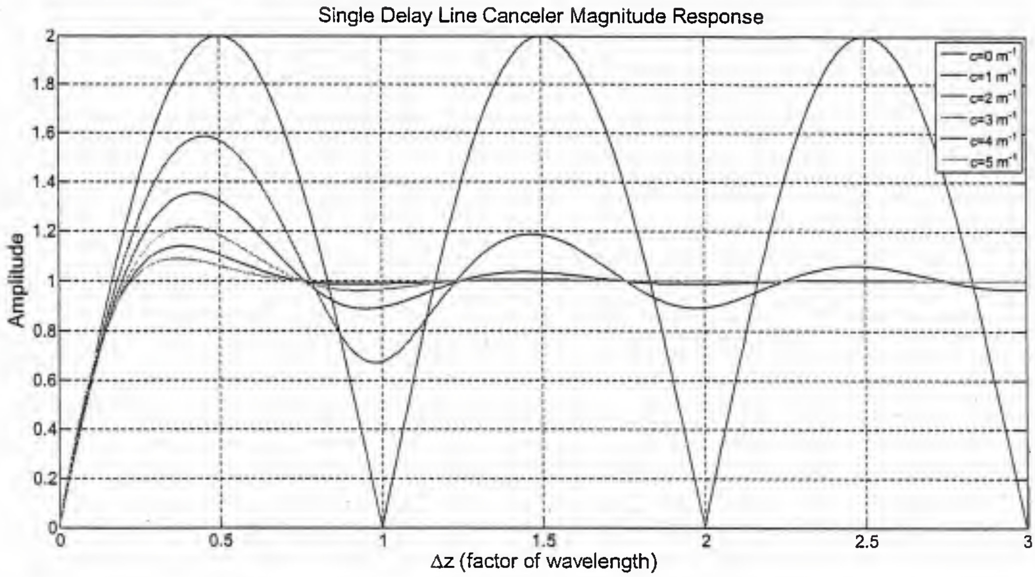

Figure 2. Magnitude response of single delay canceler for selected attenuation coefficients

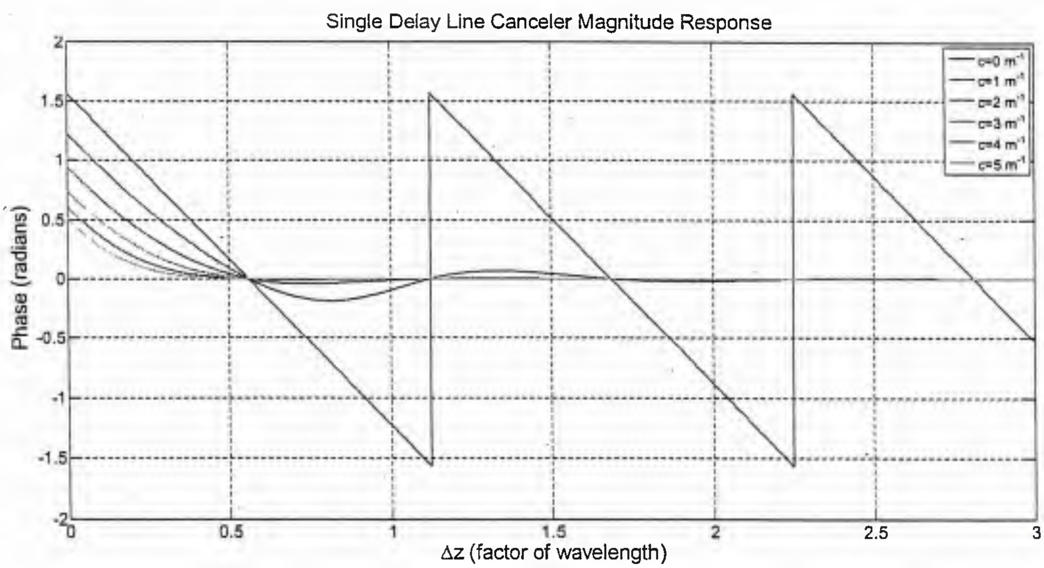

Figure 3. Phase response of single delay canceler for selected attenuation coefficients

Table 1. Optimal delays for selected attenuation coefficients

$c\ (m^{-1})$	0	1	2	3	4	5
Δz_{opt}	$0.500 * \lambda$	$0.455 * \lambda$	$0.425 * \lambda$	$0.402 * \lambda$	$0.385 * \lambda$	$0.371 * \lambda$
$M(\Delta z_{opt}, c)$	2.0	1.58	1.35	1.22	1.14	1.09
$\Phi(\Delta z_{opt}, c)$	10.00°	9.74°	6.40°	3.79°	2.15°	1.21°

The second filter explored is the double delay line canceler (also known as the triple pulse canceler). This filter was designed to have a broader rejection region in the vicinity of DC [1]. It is essentially a cascade of two single delay line cancelers in series, as shown in Figure 4. Assuming that the transmitted signal is intensity-modulated with a complex sinusoid, then the input and output signals for the double delay line canceler take the following forms:

$$S_{IN}(z,t) = e^{-cz} e^{j(\omega t - kz)}$$

$$S_{OUT}(z,t) = S_{IN}(z,t) - 2e^{-c\Delta z} S_{IN}(z+\Delta z, t) + e^{-2c\Delta z} S_{IN}(z + 2\Delta z, t)$$

With this choice for an input signal, the system transfer function H and the magnitude and phase responses can be expressed as

$$H(\Delta z, c) = 1 - 2e^{-c\Delta z}\cos(k\Delta z) + j2\sin(j\Delta z) + e^{-2c\Delta z}\cos(2k\Delta z) - je^{-2c\Delta z}\sin(2k\Delta z)$$

$$M(\Delta z, c) = \sqrt{1 + 2e^{-c\Delta z} + e^{-4c\Delta z} - \cos(k\Delta z)\left[4e^{-c\Delta z} - 4e^{-2c\Delta z}\cos(k\Delta z) + 4e^{-3c\Delta z}\right]}$$

$$\Phi(\Delta z, c) = \operatorname{atan}\left(\frac{2e^{-c\Delta z}\sin(k\Delta z) - e^{-2c\Delta z}\sin(2k\Delta z)}{1 - 2e^{-c\Delta z}\cos(k\Delta z) + e^{-2c\Delta z}\cos(2k\Delta z)}\right)$$

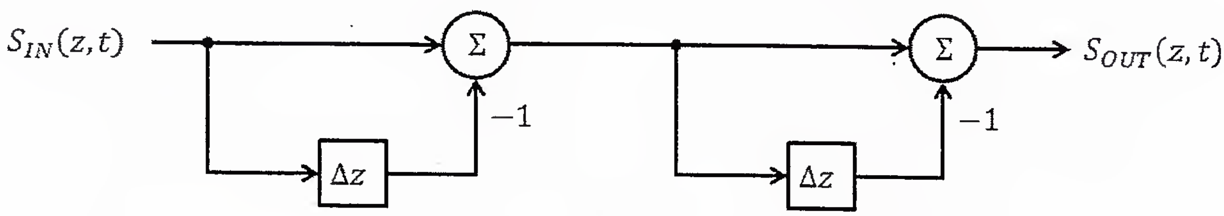

Figure 4. Double delay line canceler

The magnitude and phase responses for the double delay line canceler can be seen below in Figure 5 and Figure 6, respectively. Due to the widened cutoff region near DC for the double delay line canceler, the optimal delays have been shifted to slightly from the values seen for the single delay line canceler. As for the single delay line canceler, at the extreme case of $c = 0$, this filter reduces to the classical double delay line canceler which is periodic with period λ and suggests an optimal delay of $\Delta z_{opt} = 0.5625 * \lambda$, in the sense that this is the first point at which point the signal magnitude is most amplified. For higher values of c, the magnitude response converges towards a high-pass filter with a relatively flat passband. It is worth noting that the phase response of the double delay line canceler is not linear, even for the case $c = 0$. The optimal delay for selected values of c is summarized in Table 1, along with the magnitude gain and phase shift at these delay points.

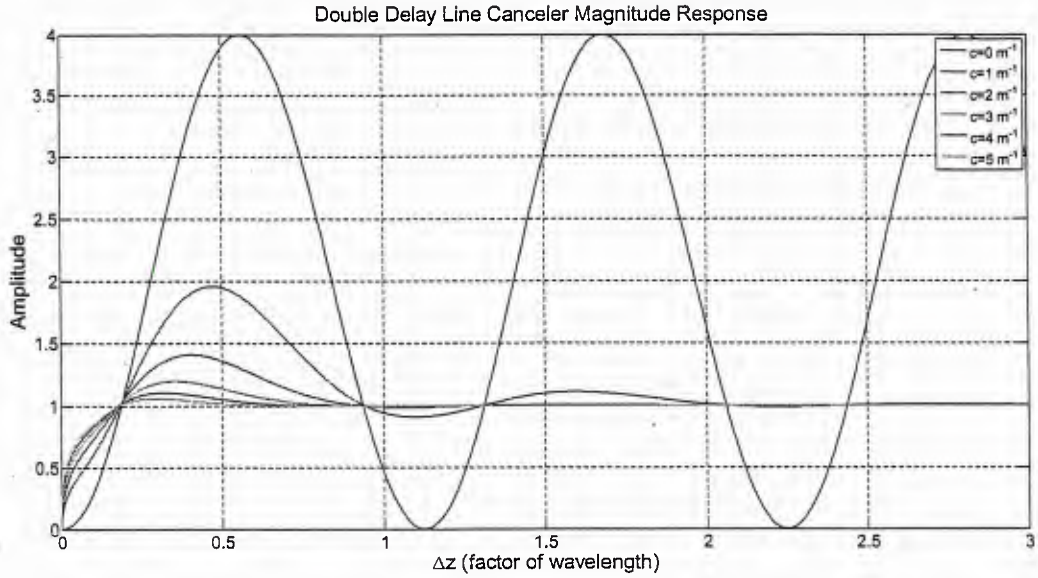

Figure 5. Magnitude response of double delay canceler for selected attenuation coefficients

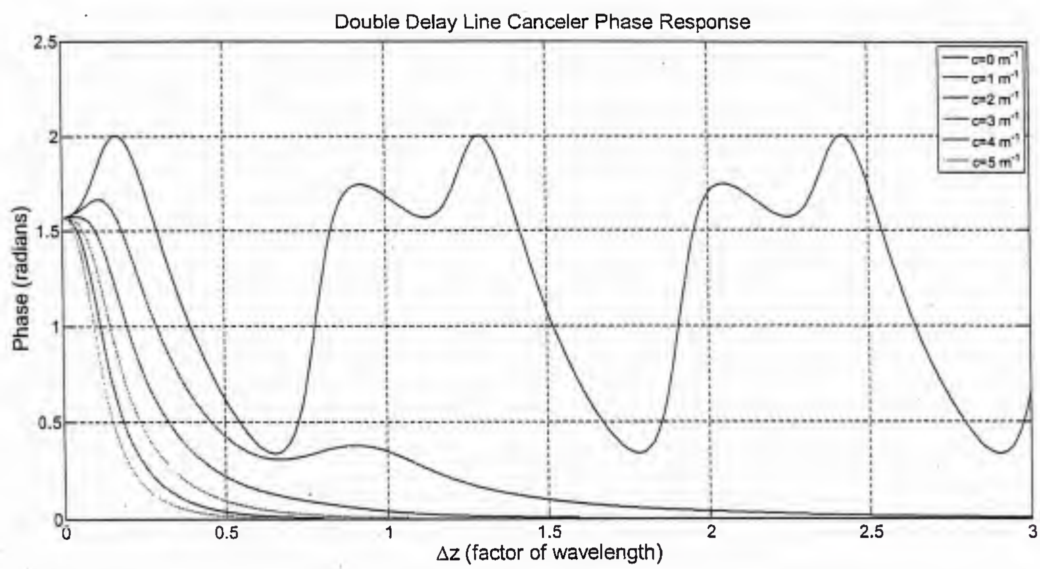

Figure 6. Phase response of double delay canceler for selected attenuation coefficients

$c\ (m^{-1})$	0	1	2	3	4	5
Δz_{opt}	$0.563 * \lambda$	$0.474 * \lambda$	$0.406 * \lambda$	$0.354 * \lambda$	$0.317 * \lambda$	$0.293 * \lambda$
$M(\Delta z_{opt}, c)$	4.00	1.96	1.41	1.20	1.11	1.06
$\Phi(\Delta z_{opt}, c)$	26.36°	26.93°	18.91°	13.18°	9.17°	6.30°

Preliminary Simulation and Experiment Results

Both the single and double delay line cancelers have been tested in simulation and on experimental data. Simulations were performed using the Underwater RangeFinder simulator produced by ATMOTOOLS [3]. RangeFinder allows the user to specify transmitter and receiver parameters, object properties, and water channel optical properties. RangeFinder was used to verify that the delay line cancelers would reduce the impact of scattering, both in terms of reducing error of ranging measurements and also by extending the useful range of the system. Experimental data was provided Dr. Linda Mullen's research group at Patuxent River Naval Air Station and was processed by the spatial filters in custom MATLAB software.

Initial experimental validation was performed using data collected at 10 centimeter intervals in a 3.6 meter long water tank at varying turbidities [4]. In this preliminary experiment, the single delay line canceler was applied to previously collected data in an attempt to reduce the ranging error. The spatial filtering delay was set to one-half of the wavelength, although this was not the optimal delay position for all turbidities used. For single-tone experiments, an improvement of a 10-20% reduction in error was observed. However, for the dual-tone experiments, the delay line canceler typically reduced ranging error by approximately 60% compared to the baseline data; for some measurements the error reduction increased to almost 80%. The single-tone approach inherently possesses higher range resolution than the dual-tone approach, while the dual-tone approach trades increased unambiguous range for reduced range resolution. Thus we would expect that spatial filtering could have a more substantial impact on a dual-tone ranging system. Indeed, it appears that spatial filtering of dual-tone data can reduce the ranging error almost to that of a single-tone approach, while still enabling the usage of the enhanced unambiguous range of the dual-tone approach.

A second set of experimental data was collected for a single-tone experiment with a modulation frequency of 140 MHz and an attenuation coefficient of $c = 1.6\ m^{-1}$ [5]. In this case, ranging was only performed over 50 centimeters with an object distance between one meter and 1.5 meters. Without filtering, the single-tone approach had an average error of 3.3 centimeters. When applying the single delay line canceler, the average error was reduced to 1.1 centimeters. The double delay line canceler was also observed to achieve a reduction in error, decreasing the average error to 1.6 centimeters. These results are substantially better than seen with the longer range experiments shown in [4]. It is possible that performance degrades somewhat for the delay line cancelers as range is increased in a single-tone system, which may account for this discrepancy.

A second analysis was performed in which the single and double delay line cancelers were used to attempt to increase the usable range of a previously collected data set. First, simulations were performed in RangeFinder for comparison to simulation results obtained without the spatial filters. This comparison is summarized in Table 2, with simulation data collected in a relatively turbid scenario of $c = 1.6\ m^{-1}$. The first three rows contain data collected without filtering shown in [6], while the spatial filtering data come from [5]. The low frequency 20 MHz single-tone is severely impacted by scattering and can be used as a baseline reference for this reason. The higher frequency single-tone extends the usable range by a factor of slightly more than two, while the dual-tone approach extends the usable range by a factor of somewhat less than two. The delay line canceler methods both extend the usable range by a factor of 2.65 compared to the baseline. In addition, this represents an increase of approximately 35% over the maximum usable range achieved in the single- and dual-tone approaches used with this particular dataset.

Table 2. Method comparison for RangeFinder simulation at $c = 1.6\ m^{-1}$

Scenario	Maximum Usable Range		Relative improvement
	Meters	Attenuation lengths	
Single-tone at 20 MHz	1.70	2.72	1.00
Single-tone at 160 MHz	3.50	5.60	2.06
Dual-tone at 160, 180 MHz	3.10	4.96	1.82
Single delay line canceler at 160 MHz	4.50	7.20	2.65
Double delay line canceler at 160 MHz	4.50	7.20	2.65

Conclusions

A class of spatial filters has been applied to extend the usable range of single- and dual-tone hybrid lidar-radar ranging systems while simultaneously reducing the error of those ranging measurements. This preliminary work has shown that the use of delay line cancelers leads to an increase in usable range of approximately 35% over single- and dual-tone systems without these filters. Additionally, reductions in error on the order of 10%-20% were observed for a single-tone system, with reductions on the order of 60% observed for a dual-tone system. These results are particularly promising considering that there are more powerful spatial filtering techniques available than those that have been used to this point, suggesting that it may be possible to realize further performance increases.

References

[1] Skolnik, Merrill I. *Introduction to Radar Systems*. 3rd ed. New York: McGraw-Hill, 2001.

[2] Yoon, Y.-S., and M.G. Amin. "Spatial Filtering for Wall-Clutter Mitigation in Through-the-Wall Radar Imaging," *IEEE Transactions on Geoscience and Remote Sensing*, vol. 47, no. 9, pp. 3192-3208, Sept. 2009.

[3] Zege, E.P., I.L. Katsev, and A.S. Prikhach. "Locating Remote Objects in Seawaters with Amplitude-Modulated Beams (RangeFinder Software)," *ATMOTOOLS*, 2011.

[4] Perez, P., W.D. Jemison, L. Mullen, and A. Laux. "Techniques to enhance the performance of hybrid lidar-radar ranging systems," *Proceedings of the IEEE OCEANS 2012 Conference*, Oct. 2012.

[5] Perez, P. *Spatial Frequency Filtering: An approach to enhancing the performance of hybrid lidar-radar ranging systems*. M.E. Report. Clarkson University: Potsdam, NY, 2013.

[6] Laux, A., L. Mullen, P. Perez, E. Zege. "Underwater Laser Range Finder," *Proceedings of SPIE 2012*.